

Host-guest Interactions in Intercalates $\text{Zr}(\text{HPO}_4)_2 \cdot 2\text{C}_2\text{H}_5\text{OH}$ and $\text{VOPO}_4 \cdot 2\text{C}_2\text{H}_5\text{OH}$

Pavla Čapková^{1,2}, Miroslava Trchová¹, Pavel Matějka³, Jiri Votinský⁴, and Henk Schenk²

¹Faculty of Mathematics and Physics Charles University Prague, Ke Karlovu 3, CZ-12116 Prague, Czech Republic. E-mail: capkova@quantum.karlov.mff.cuni.cz; trchova@mbox.troja.mff.cuni.cz

²Laboratory of Crystallography, AIMS, University of Amsterdam, Nieuwe Achtergracht 166, NL-1018 WV Amsterdam, The Netherlands. E-mail: hs@crys.chem.uva.nl; paulac@stamp.chem.uva.nl

³Department of Analytical Chemistry, Institute of Chemical Technology, Technická 5, Prague 6, CZ-16628, Czech Republic. E-mail: Pavel.Matejka@vscht.cz

⁴Department of General and Inorganic Chemistry, Faculty of Chemical Technology, University Pardubice, Naměstí legií 565, CZ-53210 Pardubice, Czech Republic. E-mail: koanch@hlb.upce.cz

Received: 26 June 1998 / Accepted: 31 August 1998 / Published: 15 September 1998

Abstract Molecular mechanics simulations using Cerius² modelling environment combined with vibrational spectroscopy (IR and Raman) have been used to study the host-guest interactions in zirconium and vanadyl phosphate intercalated with ethanol. The strategy of investigation is based on the comparison of vibrational spectra for the host compound, intercalate and guest species. This comparison confirmed the rigidity of VOPO_4 - and $\text{Zr}(\text{HPO}_4)_2$ -layers during the intercalation and provided us with the basis for the strategy of modelling. Molecular mechanics simulations revealed the structure of intercalates and enabled to analyse the host-guest interaction energy and bonding geometry. The bilayer arrangement of ethanol molecules in the interlayer space with two differently bonded ethanol molecules has been found in both intercalates. The average interaction energy ethanol-layer for two differently bonded ethanol molecules is : 127.5 and 135.7 kcal·mol⁻¹ in $\text{Zr}(\text{HPO}_4)_2 \cdot 2\text{C}_2\text{H}_5\text{OH}$, respectively 94.0 and 104.4 kcal·mol⁻¹ in $\text{VOPO}_4 \cdot 2\text{C}_2\text{H}_5\text{OH}$. The Coulombic contribution to the ethanol-layer interaction energy is predominant in all cases, but the hydrogen bonding contribution is much higher in $\text{Zr}(\text{HPO}_4)_2 \cdot 2\text{C}_2\text{H}_5\text{OH}$ than in $\text{VOPO}_4 \cdot 2\text{C}_2\text{H}_5\text{OH}$. Present results of modelling enabled the interpretation of vibrational spectra and explanation of small changes in positions and shapes of spectral bands, in infrared and Raman spectra, proceeding from the host structure to intercalates.

Keywords Vanadyl phosphate, Zirconium phosphate, Molecular mechanics, Vibrational spectroscopy, Host-guest interaction, Intercalates

Introduction

Polar organic molecules can be intercalated in the layered structure of α -zirconium and vanadyl phosphate. These intercalates are attractive materials, promising a large spectrum of applications, based on their catalytic and sorption properties, ionic conductivity, and ion exchange behavior. (For the detailed review see Clearfield [1]). The phosphate-alkanole intercalates can be considered as very good starting materials for the intercalation of other, larger polar organic molecules. Intercalation of organic molecules into the layered structure of phosphates has been studied by Clearfield [1], Alberti [2], Costantino [3] and Čapková [4,5]. All these studies showed the key role of the host-guest interactions, ruling the position of the guest molecules, their ordering in the interlayer space and the stacking of layers. Due to the strong relationship between the structure and properties in intercalates, the study of the host-guest interactions is very important for the understanding and prediction of their properties.

Present work is a continuation of our recent structure analysis of two intercalates: $\text{Zr}(\text{HPO}_4)_2 \cdot 2\text{C}_2\text{H}_5\text{OH}$ [4] and $\text{VOPO}_4 \cdot 2\text{C}_2\text{H}_5\text{OH}$ [5], based on the combination of molecular mechanics simulations and X-ray diffraction. These recent works present the detailed structure analysis, including the characterization of structural disorder. Results of structure analysis confirmed the significance of the host-guest interaction for the structure-properties relationship in intercalates and showed also the importance of vibrational

spectroscopy for this study. The combination of molecular mechanics simulation using Cerius² with infrared (IR) and Raman spectroscopy, has been used in the present study of host-guest interaction in vanadyl and zirconium phosphates, intercalated with ethanol. The strategy of investigation is based on the comparison of vibrational spectra for host compound, intercalate and guest species. This comparison is a good starting point for the modelling strategy. On the other hand the results of molecular simulations enable the interpretation of changes in spectral bands, proceeding from the vibrational spectra of host compounds and guest species to spectra of intercalates. Thus the combination of molecular simulations with infrared and Raman spectroscopy represents a very powerful tool for investigation of changes in structure and bonding during intercalation.

Spectroscopic measurements and modelling strategy

The method of sample preparation has already been described in our previous papers [4,5]. Infrared measurements were carried out using a NICOLET IMPACT 400 Fourier transform infrared (FTIR) spectrophotometer in a H_2O -purged environment. An ambient-temperature deuterated triglycine sulphate (DTGS) detector was used for the wavelength range from 400 to 4000 cm^{-1} . A Happ-Genzel apodization function was used in all region and the spectral resolution was 2 cm^{-1} . The Baseline Horizontal Attenuated Total Reflection (HATR)

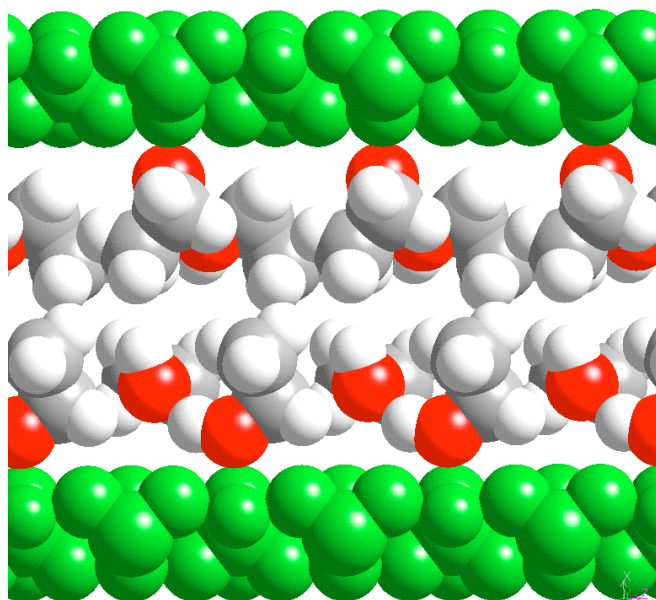


Figure 1a Packing of ethanol molecules in the interlayer space of vanadyl phosphate. The VOPO_4 layers are green. One half of the total number of ethanol molecules is anchored at vanadium to complete V-octahedra

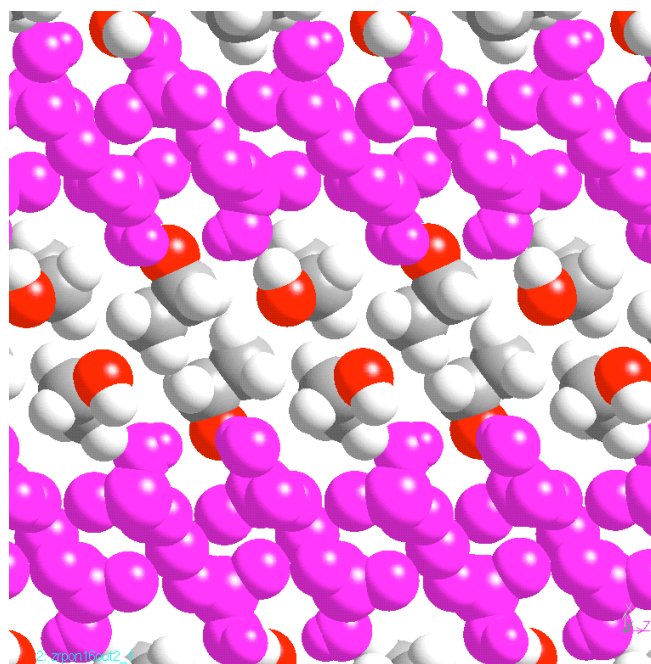


Figure 1b Packing of ethanol molecules in the interlayer of α -zirconium phosphate. The partial overlap of $\text{Zr}(\text{HPO}_4)_2$ layers (purple color) with ethanol layers is evident

Table 1 The values of Van der Waals (VDW), Coulombic (COUL) and hydrogen bonding (H-B) contributions to the total interaction energy ethanole-layer in both intercalates

Energy (kcal)		VDW	COUL	H-B	Total
Zr(HPO ₄) ₂ ·2C ₂ H ₅ OH	ethanole 1	4.6	119.9	3.0	127.5
	ethanole 2	1.6	124.0	10.1	135.7
VOPO ₄ ·2 C ₂ H ₅ OH	ethanole 1	0.9	102.8	0.6	104.4
	ethanole 2	3.9	89.5	0.6	94.0

accessory with ZnSe crystal was used for measurements of infrared spectra of host structures, intercalates and pure ethanole.

FT Raman spectra were collected using a Fourier transform near-infrared (FT-NIR) spectrometer Equinox 55/S (Bruker) equipped with FT Raman module FRA 106/S (Bruker). The samples were irradiated by the focused laser beam with a laser power 100mW of Nd-YAG laser (1064 nm, Coherent). The scattered light was collected in back scattering geometry. Quartz beamsplitter and Ge detector (liquid N₂ cooled) were used to obtain interferograms. 128 interferograms were co-added and then processed by the Fourier transformation Blackman-Harris 4-term apodization a zerofilling factor 8 to obtain final FT Raman spectra in the range 4000 – (–1000) cm^{–1} with 4 cm^{–1} resolution.

Strategy of modelling is described in details in [4,5]. The replacement of the water molecules with ethanole in the *a*-ZrP interlayer during intercalation leads to the assumption, that the host-guest interactions in this intercalate can be described by the non-bond terms only, that means the Crystal Packer Module in Cerius² modelling environment can be used. Using Crystal Packer we have to assume the rigid layers and rigid ethanole molecules. Both these assumptions are supported by the vibrational spectroscopy and by the fact, that the water molecules can be replaced by ethanole reversibly.

Crystal Packer is a computational module which estimates the total sublimation energy and packing of molecular crystals. Energy calculations in Crystal Packer take into account the non-bond terms only, i.e. van der Waals interactions (VDW), Coulombic interactions (COUL), hydrogen bonding (H-B), internal rotations and hydrostatic pressure. The asymmetric unit of the crystal structure is divided into rigid units. Non-bond (VDW, COUL, H-B) energies are calculated between the rigid units. During the energy minimization, the rigid units can be translated and rotated and the unit cell parameters varied. In all initial models built in the present work, the rigid units were ethanole molecules and Zr(HPO₄)₂-layer resp. VOPO₄-layer.

For VDW we used the well known Lennard-Jones functional form, with the arithmetical radius combination rule. The non-bond cut-off distance for the VDW interactions was 7.0 Å. From the 3 force fields available in Crystal packer module: Dreiding, Universal and Tripos, the Dreiding force field [6] has been found as the best one for the description of VDW forces between the rigid units in our model. As the Dreiding force field available in Cerius² has no VDW param-

eters for zirconium and vanadium, we add Zr- and V-parameters for VDW term those taken from the Universal force field. (For the detailed description of the Dreiding force field see work Mayo et al. [6] and Universal force field is described in [16]). Hydrogen bond term was CHARM-like angle dependent potential, with Dreiding coefficients. The Ewald summation method is used to calculate the Coulombic energy in a crystal structure [7]. Ewald sum constant was 0.5 Å^{–1}. Minimum charge taken into Ewald sum was 0.00001e. All atom pairs with separation less than 10 Å were included in the real-space part of the Ewald sum and all reciprocal-lattice vectors with lengths less than 0.5 Å^{–1} were included in the reciprocal part of the Ewald summation. Charges in crystal are calculated in Cerius² using QEq-method (Charge equilibrium approach). This methods is described in details in the original work [8]. The external pressure 99 kbar has been applied for the first minimization of the initial model and then the external pressure was removed and new minimization started.

Modeling results

The complete structure analysis of VOPO₄·2C₂H₅OH and Zr(HPO₄)₂·2C₂H₅OH based on combination of molecular mechanics simulations and X-ray diffraction has been carried out in our previous works [4,5], in which the detailed description of structure has been presented including: positions and orientations of ethanole molecules with respect to layers, the crystal packing of ethanole molecules in bilayer arrangement in the interlayer space and including the stacking of layers. Molecular simulations also enabled to describe the disorder in positions and orientations of ethanole molecules and disorder in layer stacking in both intercalates.

The present work will be focused in more details to host-guest interactions, i.e. to the anchoring of ethanole molecules to the host layers and to the bonding layer-ethanole, with special attention to hydrogen bonds, affecting the IR spectra. The results of modelling will be used for the interpretation of vibrational spectra of both intercalates, that means for the changes in spectral bands (their positions and shapes), proceeding from the host structure to the intercalate.

Both intercalates exhibit certain common structural features, which can be summarized in following items:

Bilayer arrangement of ethanoles in the interlayer.

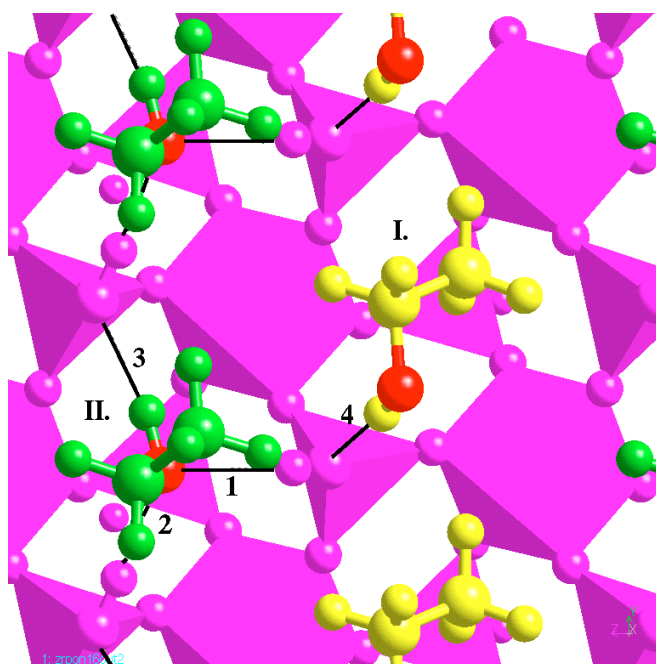


Figure 2a Positions of two differently bonded ethanol molecules in the pseudohexagonal cavities on the $Zr(HPO_4)_2$ layers (purple) in the intercalate $Zr(HPO_4)_2 \cdot 2C_2H_5O$ found by molecular mechanics simulations. Cavities I. and II. have differently oriented P-OH groups and consequently different hydrogen bonding scheme of ethanoles (ethanole oxygens are red). Two distinct P-OH groups exhibit different hydrogen bond geometry with ethanol: (a) hydrogen bridges 2 and 3 pointing to the first P-OH group and (b) hydrogen bridges 1 and 4 pointing the second P-OH group

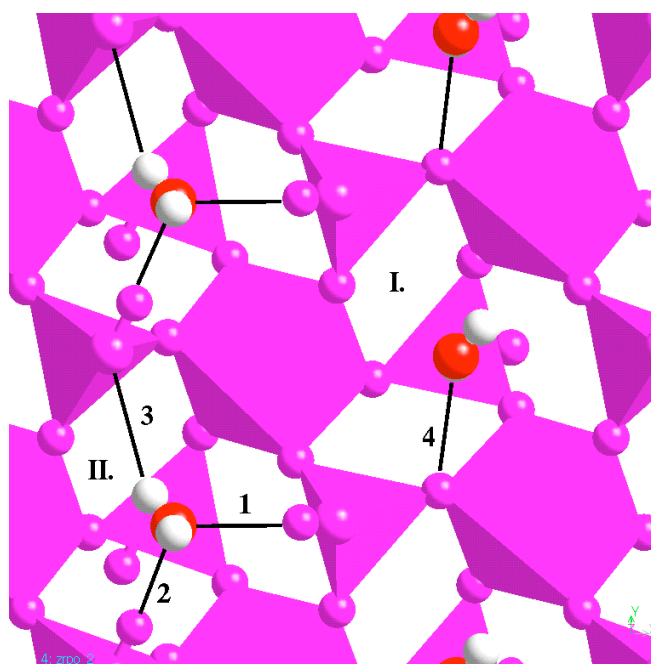


Figure 2b Position of water molecules in cavities on the $Zr(HPO_4)_2$ layers (purple) in the host structure the $Zr(HPO_4)_2 \cdot H_2O$, according to Troup & Cliefeld [10]. All water molecules are linked via 3 hydrogen bridges to P-OH groups and via one hydrogen bridge to the shared oxygen Zr-O-P

In both intercalates there are two distinct types of ethanol molecules, which are differently bonded to the layers.

In both intercalates we observed certain degree of disorder in positions and orientations of ethanol molecules, resulting in the certain degree of disorder in layer stacking.

The difference in crystal packing, arising from the different structure of $VOPO_4$ and $Zr(HPO_4)_2$ layers can be seen in figures 1a,b. In case of $VOPO_4$ the layer surface is flat and the ethanol layers touch upon the $VOPO_4$ layers only via the ethanol oxygens. (See figure 1a, note that only one half from the total number of ethanol molecules is anchored to the $VOPO_4$ layers!). In case of α -zirconium phosphate, the ethanol molecules sit in the cavities in $Zr(HPO_4)_2$ layers and the ethanol molecules are slightly immersed in the adjacent host layers and one can see the closer packing in the interlayer space of $Zr(HPO_4)_2 \cdot 2C_2H_5OH$.

Two different PO_4 groups in the lattice of α -zirconium phosphate reported already by Clearfield & Smith [9], result in two different types of cavities in $Zr(HPO_4)_2$ layers, denoted as I and II (see figure 2a). In cavity I all OH-groups in three adjacent (HPO_4) tetrahedra are pointed out of the cavity, while in case of cavity II, two OH-groups are directed inside the cavity. As one can see in figure 2a, two differently

bonded ethanol molecules reside in both cavities. Ethanol 1 (yellow) in cavity I is bound by one hydrogen bond to the OH-group of $Zr(HPO_4)_2$ layer. Ethanol 2 (green) in cavity II creates 3 hydrogen bridges to OH-groups of adjacent (HPO_4) tetrahedra. The values of interaction energy ethanol-layer for both ethanol molecules are in table 1, where one can see the Van der Waals, Coulomb and hydrogen bonding contributions to the total interaction energy and the differences for ethanoles in cavity I and II. The energy values presented in table 1 represents the average values calculated from the series of minimized models. All these minimized models exhibited the behaviour characteristic for disordered structures, i.e. slightly different positions and orientations of ethanol molecules and nearly the same sublimation energy [4].

Figure 2b illustrates the arrangement of water molecules in the host compound $Zr(HPO_4)_2 \cdot H_2O$, according to the structure data published by Troup & Clearfield [10]. Comparing the figures 2a and 2b, we can see the similar way of anchoring to layers for water and ethanol molecules. Both are sitting in the cavities, with different hydrogen bonding scheme in the cavity I and II. As the water molecules are arranged in one layer in the interlayer space of $Zr(HPO_4)_2 \cdot H_2O$, each water molecule is involved in 4 hydrogen bonding to both adjacent

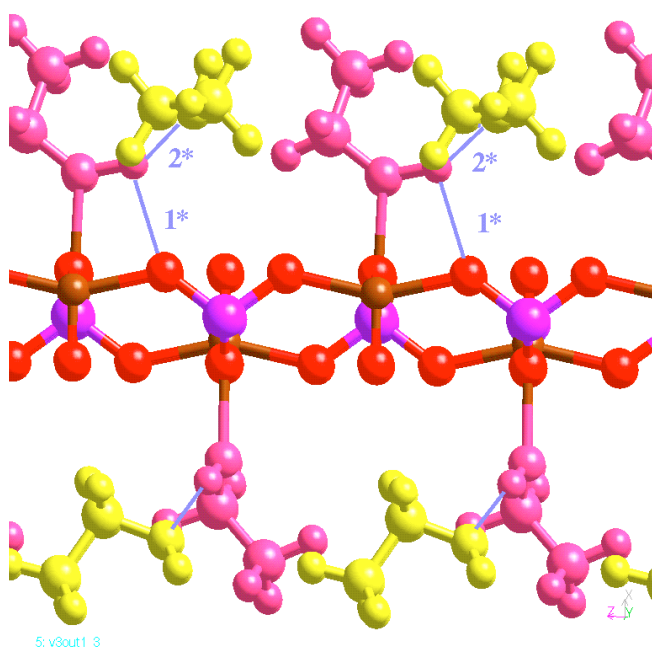


Figure 3a Two differently bonded ethanol molecules (pink and yellow) in the interlayer of $\text{VOPO}_4 \cdot 2\text{C}_2\text{H}_5\text{OH}$. The first ethanol (pink) is attached to vanadium to complete V-octahedron, the second ethanol (yellow) is hydrogen bonded to the attached one. Both ethanols create only sporadically hydrogen bridges with layer oxygens (hydrogen bridges are marked with blue solid lines 1*, 2*)

layers: in cavity I, three hydrogen bonds to lower $\text{Zr}(\text{HPO}_4)_2$ layer and one to the upper layer, in cavity II the hydrogen bonding scheme has opposite orientation, (i.e. one hydrogen bond to lower and three to upper layer). As it is evident from comparison of figures 2a and 2b, the hydrogen bonding scheme is very similar in case of the host structure $\text{Zr}(\text{HPO}_4)_2 \cdot \text{H}_2\text{O}$ and intercalate $\text{Zr}(\text{HPO}_4)_2 \cdot 2\text{C}_2\text{H}_5\text{OH}$. Anyway the geometry of hydrogen bonding is of course slightly different and the main difference is between the bonding of P-OH groups to interlayer molecules. In the intercalate $\text{Zr}(\text{HPO}_4)_2 \cdot 2\text{C}_2\text{H}_5\text{OH}$, both distinct P-OH groups are involved in two hydrogen bonds with ethanol molecules, whereas in the host structure $\text{Zr}(\text{HPO}_4)_2 \cdot \text{H}_2\text{O}$ one P-OH group is involved in two hydrogen bonds and the second one only in one hydrogen bond. Water molecules are hydrogen bonded also to shared Zr-O-P oxygens, as one can see from the figure 2b (H-bridge no.4).

In $\text{VOPO}_4 \cdot 2\text{C}_2\text{H}_5\text{OH}$, two differently bonded ethanol molecules are shown in figure 3a. Ethanol 1 (pink) is located above and below the vanadium atom to complete the vanadium octahedra. Ethanol 2 (yellow), which is more loosely bonded in the interlayer space (see table 1) is hydrogen bonded to the ethanol 1. Both ethanol molecules create only sporadically the hydrogen bridges to VOPO_4 layers (either to PO_4 oxygens or to $\text{V}=\text{O}$ oxygens), consequently the average hydrogen bonding energy ethanol-layer is very

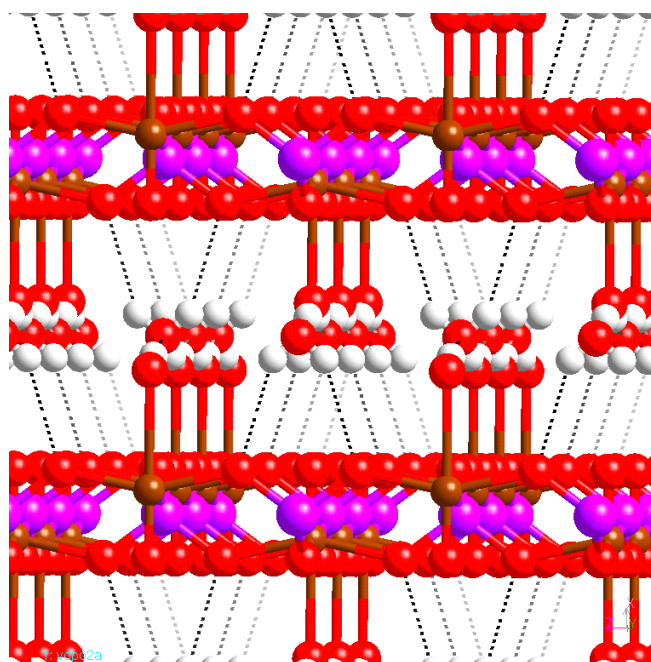


Figure 3b The arrangement of water molecules in the interlayer of the host structure $\text{VOPO}_4 \cdot 2\text{H}_2\text{O}$. The network of hydrogen bonds is marked with dotted lines

low in comparison with $\text{Zr}(\text{HPO}_4)_2 \cdot 2\text{C}_2\text{H}_5\text{OH}$ intercalate. As it is evident from table 1, predominant Coulombic contribution to host-guest interaction is characteristic of both intercalates, however ethanol molecules are more loosely bonded in $\text{VOPO}_4 \cdot 2\text{C}_2\text{H}_5\text{OH}$ than in $\text{Zr}(\text{HPO}_4)_2 \cdot 2\text{C}_2\text{H}_5\text{OH}$. Figure 4 shows the view along the direction perpendicular to VOPO_4 layer, illustrating the arrangement of adjacent ethanol molecules.

Figure 3b shows the crystal packing in the interlayer space of the host compound according to structure data of Tachez et al. [11]. The network of hydrogen bonds is marked with dotted lines. One can see the regular system of hydrogen bonds between the second more loosely bonded water molecule and PO_4 oxygens. The second hydrogen bond system between two distinct water molecules is pointed along the direction perpendicular to the plane of projection and is hidden in figure 3b. Comparison of figures 3a and 3b shows clearly the common features and difference between the bonding of water and ethanol molecules to the VOPO_4 layers:

the oxygen of the first water molecule is bonded to vanadium atom (the bond distance O-V $\sim 2.2335 \text{ \AA}$ for H_2O [12] and 2.50 \AA for D_2O [11]). The same way of anchoring to the VOPO_4 layer occur in case of ethanol 1, with the average V-O distance obtained from modelling $\sim 2.38 \text{ \AA}$. Both molecules, water and ethanol, involved in the vanadium octahedron are hydrogen bonded to neighbouring interlayer molecules.

Table 2a Positions of the main spectral bands in Raman spectrum of $Zr(HPO_4)_2 \cdot H_2O$ and $Zr(HPO_4)_2 \cdot 2C_2H_5OH$. Vibration mode symbols have been used in agreement with the book of Ross [13]

Vibration modes : Raman	$\nu_1(A_1)$ - symmetric stretching HPO_4	$\nu_3(F_2)$ - antisym. stretching HPO_4	δ_{POH} - out of plane deformation mode
$Zr(HPO_4)_2 \cdot H_2O$	1078 cm^{-1} 1053 cm^{-1}	1138 cm^{-1}	985 cm^{-1} 960 cm^{-1}
$Zr(HPO_4)_2 \cdot 2C_2H_5OH$	1065 cm^{-1} 1053 cm^{-1}	1147 cm^{-1}	978 cm^{-1} 952 cm^{-1}

The difference is in the bonding of the second water molecule and ethanole 2 to the $VOPO_4$ layers. While the second water molecule is hydrogen bonded equally through both hydrogens to the PO_4 tetrahedra, the ethanole 2 (yellow) is hydrogen bonded only to the ethanole 1. The analysis of a series of minimized models showed, that both ethanoles 1 and 2 may sporadically create hydrogen bridges either to PO_4 oxygens or to $V=O$ oxygens. Consequently the average contribution of hydrogen bond energy to the total interaction energy ethanole-layer is very low in $VOPO_4 \cdot 2C_2H_5OH$ compared with $Zr(HPO_4)_2 \cdot 2C_2H_5OH$, as one can see in table 1.

Vibrational spectra and their relation to the structure of intercalates

α -zirconium phosphate intercalated with ethanole

Figure 5a shows the comparison of Raman spectra of the host structure $Zr(HPO_4)_2 \cdot H_2O$, ethanole and intercalate $Zr(HPO_4)_2 \cdot 2C_2H_5OH$. It is evident, that all spectral bands corresponding to the vibrations of $Zr(HPO_4)_2$ layer observable in Raman spectrum of the host structure are observable also in the spectrum of intercalated structure. The difference in positions of corresponding bands in host structure and intercalate is very small (see table 2a). That means, the $Zr(HPO_4)_2$ layers are rigid during intercalation and the assumption of rigid layers in modelling represents a reasonable approximation in case of α -zirconium phosphate, intercalated with ethanole. The small peak shifts and intensity redistribution in Raman spectra of $Zr(HPO_4)_2 \cdot 2C_2H_5OH$ in comparison with host compound are due to the replacement of water by ethanole in cavities I and II. This replacement will affect both: stretching HPO_4 modes and deformation P-O-H modes, due to the different scheme of hydrogen bonding between P-OH and water and between P-OH and ethanoles (compare figures 2a and 2b). The rather pronounced change in shape of two bands corresponding to $\nu_1(A_1)$ - HPO_4 symmetric stretching can be partially attributed to the overlap with the ethanole bands (see the lowest spectrum in the figure 5a).

The IR spectra of $Zr(HPO_4)_2 \cdot H_2O$, $Zr(HPO_4)_2 \cdot 2C_2H_5OH$ and ethanole are compared in figures 5b and band positions are summarised in table 2b. The IR spectra exhibit the same

character for the host structure and intercalate, with the small or negligible shift of band positions and small changes of band profiles due to the intensity redistribution in the spectrum of intercalate. These small changes are consistent with the frequency shifts, observed in Raman spectra of $Zr(HPO_4)_2 \cdot 2C_2H_5OH$, as a consequence of different hydrogen bonding between P-OH and ethanole molecule in the intercalate and between P-OH and water molecule in the host structure, as it is evident from comparison of figures 2a and 2b.

Comparing the position of ethanole bands in IR and Raman spectra of intercalate $Zr(HPO_4)_2 \cdot 2C_2H_5OH$ with those for pure ethanole (figures 5a and 5b), we can see a slight shift of ethanole bands to lower wave numbers in case of intercalate. This slight shift is due to the anchoring of ethanole molecules in the layer cavities, resulting in closer crystal packing and stronger host-guest interaction energy for $Zr(HPO_4)_2 \cdot 2C_2H_5OH$ than for $VOPO_4 \cdot 2C_2H_5OH$, especially in case of hydrogen bonding (see table 1). This ethanole peak

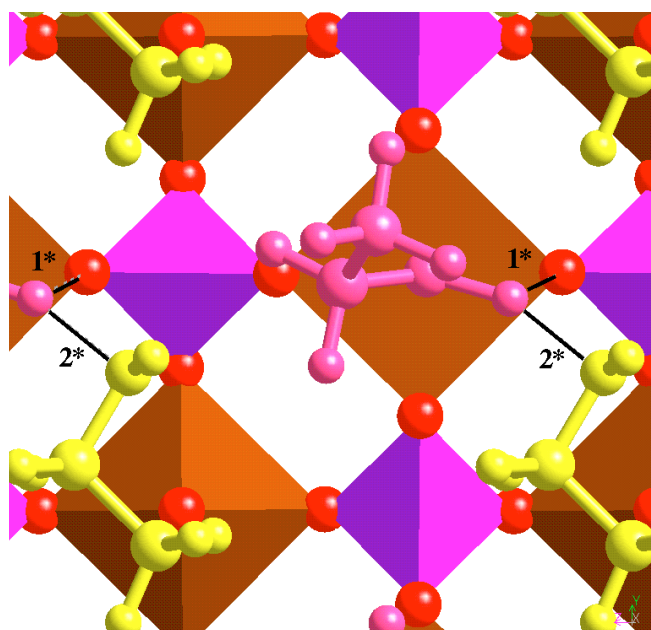
**Figure 4** The arrangement of ethanole molecules above the $VOPO_4$ layer

Table 2b Positions of the main absorption bands in IR spectrum of $Zr(HPO_4)_2 \cdot H_2O$ and $Zr(HPO_4)_2 \cdot 2C_2H_5OH$

Vibration modes : IR	$\nu_1(A_1)$ HPO_4 symmetric stretching	$\nu_3(F_2)$ HPO_4 antisym. stretching	δ_{POH} - in plane deformation mode	δ_{POH} - out of plane deform. mode
$Zr(HPO_4)_2 \cdot H_2O$	1070 cm^{-1} 1045 cm^{-1} 1032 cm^{-1}	1162 cm^{-1} 1122 cm^{-1}	1249 cm^{-1}	967 cm^{-1} 957 cm^{-1}
$Zr(HPO_4)_2 \cdot 2C_2H_5OH$	1059 cm^{-1} 1045 cm^{-1} 1037 cm^{-1}	1162 cm^{-1} (w) 1122 cm^{-1} (vw)	1249 cm^{-1}	964 cm^{-1} 946 cm^{-1}

w - weak band, vw - very weak band

shift is not observable in case of $VOPO_4 \cdot 2C_2H_5OH$, where the host-guest interaction energy is lower than in $Zr(HPO_4)_2 \cdot 2C_2H_5OH$ (see table 1).

Vanadyl phosphate intercalated with ethanol

Comparison of Raman spectra for the host structure $VOPO_4 \cdot 2H_2O$ and intercalate $VOPO_4 \cdot 2C_2H_5OH$ in the figure 6a illustrates the rigidity of $VOPO_4$ layers during intercalation. The ethanol bands in the Raman spectrum of intercalate $VOPO_4 \cdot 2C_2H_5OH$ were exactly in the same positions as in the spectrum of pure ethanol. Consequently the ethanol spectrum can be subtracted from the spectrum of intercalate.

As a result of this subtraction we have got the spectrum of intercalate without ethanol bands, (see figure 6a), which is more convenient for the comparison of bands corresponding to $VOPO_4$ layers in host and intercalated structure. Table 3a summarises the positions of the main spectral bands in both Raman spectra and one can see in the table 3a and figure 5b, that the Raman spectrum is almost the same for the host structure and intercalate. Three bands observable at 1035, 1014 and 985 cm^{-1} in the Raman spectrum of the host structure correspond to the $V=O$ stretching mode. The vanadyl stretching band is especially sensitive to the local coordination of vanadium and three peaks indicate the presence of anhydrous, partially and fully hydrated form of $VOPO_4$. This partial escape of water is due to the laser beam during the measure-

Figure 5a Raman spectra of the host structure $Zr(HPO_4)_2 \cdot H_2O$, intercalate $Zr(HPO_4)_2 \cdot 2C_2H_5O$ and ethanol

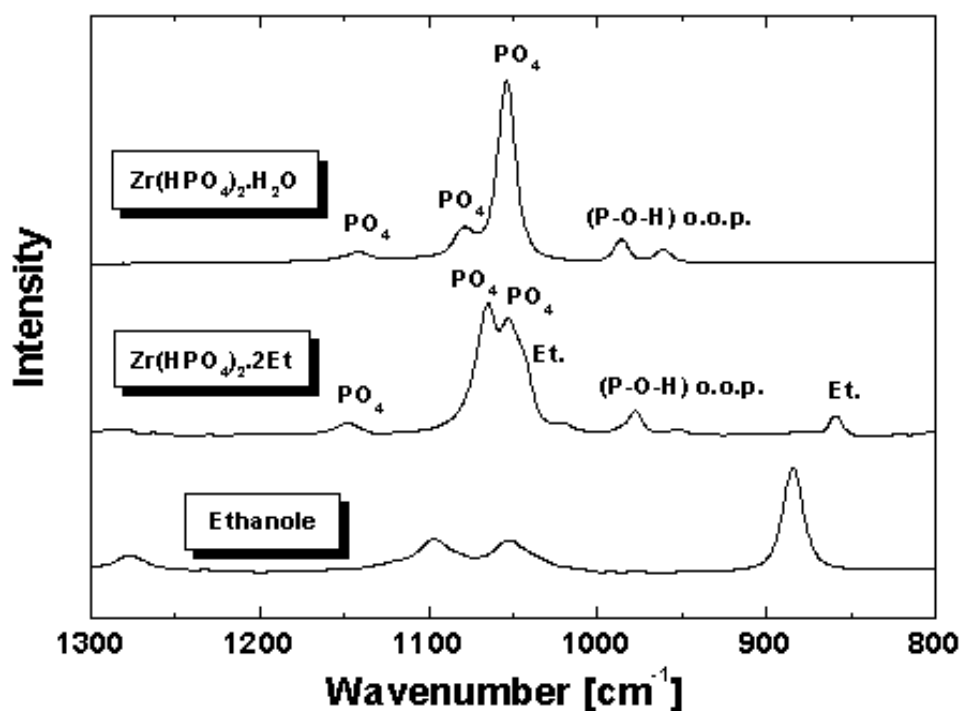


Table 3a Positions of the main spectral bands in Raman spectra of the host structure $\text{VOPO}_4 \cdot 2\text{H}_2\text{O}$ and intercalate $\text{VOPO}_4 \cdot 2\text{C}_2\text{H}_5\text{OH}$

Vibration modes: Raman	ν V=O stretching	$\nu_1(\text{A}_1)$ PO_4 symmetric stretching	$\nu_4(\text{F}_2)$ PO_4 symmetric bending	$\nu_2(\text{E})$ PO_4 antisym. bending
$\text{VOPO}_4 \cdot 2\text{H}_2\text{O}$	1035 cm^{-1} 1014 cm^{-1} (vw) 985 cm^{-1}	945 cm^{-1} (s) 929 cm^{-1} (sh)	579 cm^{-1} 541 cm^{-1}	460 cm^{-1}
$\text{VOPO}_4 \cdot 2\text{C}_2\text{H}_5\text{OH}$	1029 cm^{-1} (b) 990 cm^{-1}	937 cm^{-1} (s)	572 cm^{-1} (vw) 529 cm^{-1}	460 cm^{-1}

b - broad, *s* - strong, *sh* - shoulder, *vw* - very weak band

ments. (for more detailed explanation see [17]). In case of intercalate $\text{VOPO}_4 \cdot 2\text{C}_2\text{H}_5\text{OH}$ these bands are slightly shifted and very broaden. This broadening of V=O bands reflects the disorder in positions of ethanole molecules found by molecular simulations. Due to the slight disorder in positions and orientations of ethanole molecules in the interlayer space of $\text{VOPO}_4 \cdot 2\text{C}_2\text{H}_5\text{OH}$, described in our previous work [5], the bond distance $\text{V-O}_{\text{ethanole}}$ varies within the range 2.26 – 2.50 Å giving the average value ~ 2.38 Å. These fluctuating $\text{V-O}_{\text{ethanole}}$ bond distances exhibit different effect on adjacent V=O bonds, resulting in broadening of spectral bands.

The second consequence of the disorder in the ethanole arrangement in the interlayer of $\text{VOPO}_4 \cdot 2\text{C}_2\text{H}_5\text{OH}$ is the irregularity in the hydrogen bonding of ethanole molecules to

PO_4 oxygens. Results of modelling showed, that the regular network of hydrogen bonds observable in host compound (see figure 3b) is never present in the intercalate. Only few irregularly arranged hydrogen bridges between ethanole and VOPO_4 -layer have been observed in the series of calculated structure models (see figure 3a). This irregularity in hydrogen bonding of ethanoles to PO_4 oxygens affects the PO_4 stretching and bending modes, as one can see in table 3a and figure 6a. In spite of the small differences in Raman spectra of host structure and intercalate $\text{VOPO}_4 \cdot 2\text{C}_2\text{H}_5\text{OH}$ discussed above, the character of both spectra remain the same supporting the assumption of rigid VOPO_4 layers and rigid ethanole during intercalation.

Figure 5b IR spectra of the host structure $\text{Zr}(\text{HPO}_4)_2 \cdot \text{H}_2\text{O}$, intercalate $\text{Zr}(\text{HPO}_4)_2 \cdot 2\text{C}_2\text{H}_5\text{O}$ and ethanole

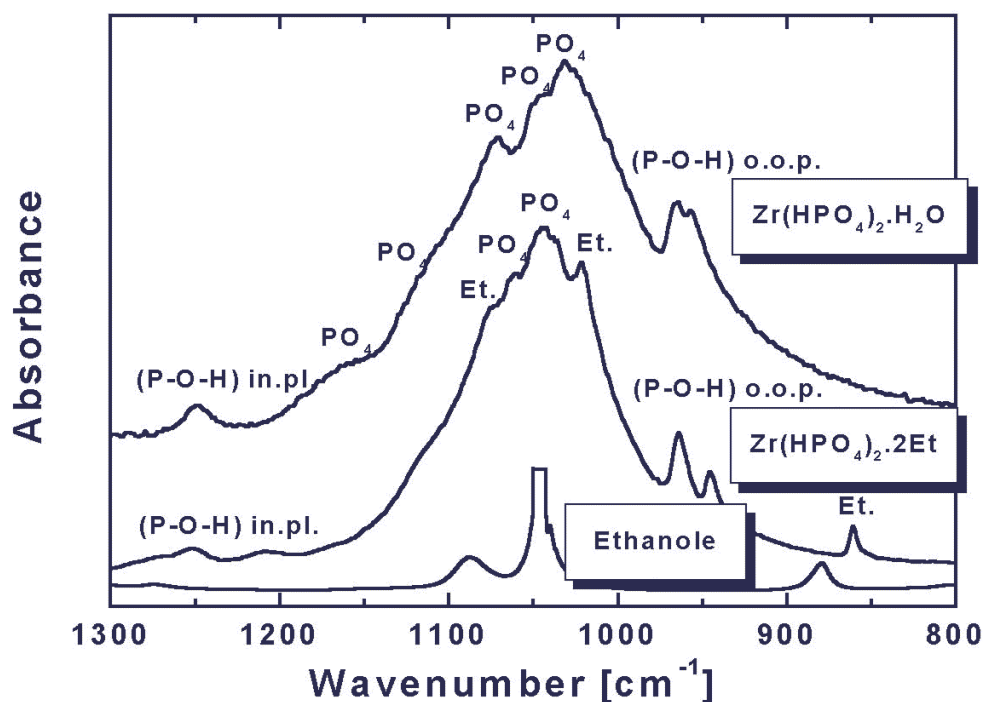


Table 3b Positions of the main absorption bands in IR spectra of the host structure $\text{VOPO}_4 \cdot 2\text{H}_2\text{O}$ and intercalate $\text{VOPO}_4 \cdot 2\text{C}_2\text{H}_5\text{OH}$

Vibration modes: IR	$\nu_3(\text{F}_2) \text{ PO}_4$ antisymm. stretching	$\nu \text{ V=O}$ stretching	Mixed: $\nu_1(\text{PO}_4)$, $\delta(\text{P-O-V})$, $\rho(\text{H}_2\text{O})$	lattice vibr.
$\text{VOPO}_4 \cdot 2\text{H}_2\text{O}$	1143 cm^{-1} 1076 cm^{-1} (w)	995 cm^{-1}	cg = 920 cm^{-1}	681 cm^{-1}
$\text{VOPO}_4 \cdot 2\text{C}_2\text{H}_5\text{OH}$	1143 cm^{-1} ethanole band overlap	995 cm^{-1} (w)	cg = 920 cm^{-1}	681 cm^{-1}

vw - very weak band , *cg* - center of gravity of mixed absorption band

IR spectra of the host structure, intercalate and ethanole are in figure 6b. One can easily identify the bands corresponding to the ethanole molecules. In contradiction to $\text{Zr}(\text{HPO}_4)_2 \cdot 2\text{C}_2\text{H}_5\text{O}$, the ethanole bands keep the same positions in intercalate $\text{VOPO}_4 \cdot 2\text{C}_2\text{H}_5\text{OH}$ as in the pure ethanole. This is due to the very weaker bonding ethanole-layer. Comparing the IR spectrum of $\text{VOPO}_4 \cdot 2\text{H}_2\text{O}$ and $\text{VOPO}_4 \cdot 2\text{C}_2\text{H}_5\text{OH}$ we can see all the bands occurring in host structure, also in the intercalate even in the same positions, see table 3b. The broaden band in the spectrum of host structure with the center of gravity at $\sim 920 \text{ cm}^{-1}$ contains the mixture of overlapping bands: $\nu_1(\text{PO}_4)$, $\delta(\text{P-O-V})$ and $\rho(\text{H}_2\text{O})$. It is evident, that this band should change it's profile, proceeding from the host structure to intercalate, because of:

$\rho(\text{H}_2\text{O})$ are absent in the intercalate

$\delta(\text{P-O-V})$ deformation bands are suppressed in the intercalate due to the small amount of hydrogen bridges between ethanole and layers, in comparison with the network of hydrogen bridges in host structure see figures 3a,b.

Conclusions

Present results showed, that the combination of molecular simulations with IR and Raman spectroscopy is very useful in analysis of structure and bonding in intercalates. The main reasons for the use of vibrational spectroscopy in complex structure analysis can be summarized in the following two main points:

Figure 6a Raman spectra of the host structure $\text{VOPO}_4 \cdot 2\text{H}_2\text{O}$ and intercalate $\text{VOPO}_4 \cdot 2\text{C}_2\text{H}_5\text{OH}$, where the ethanole spectrum has been subtracted

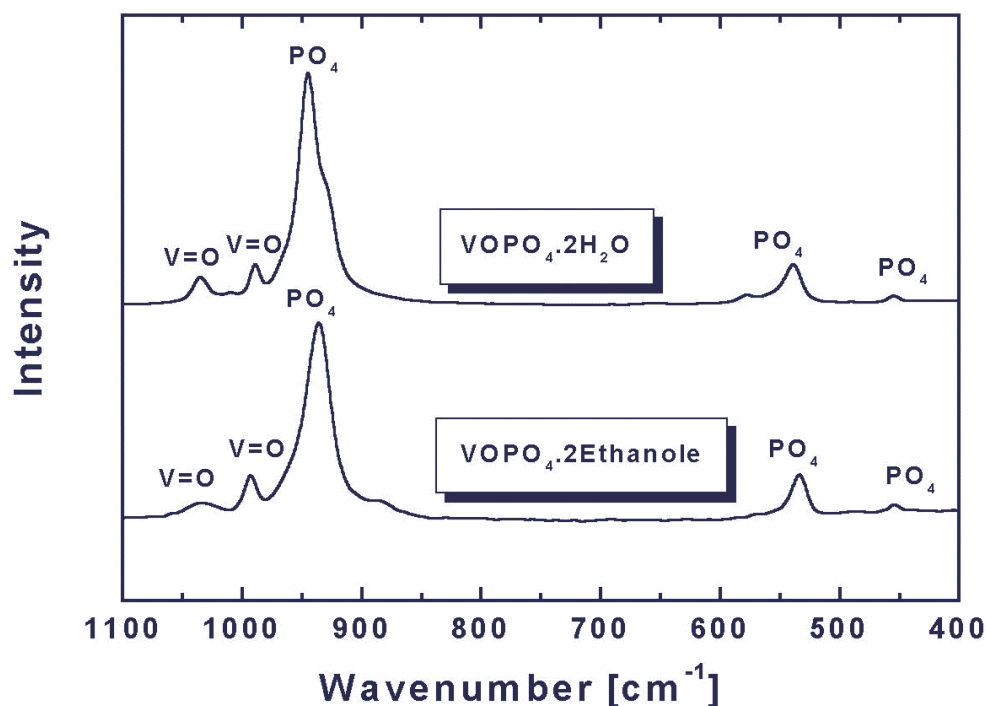
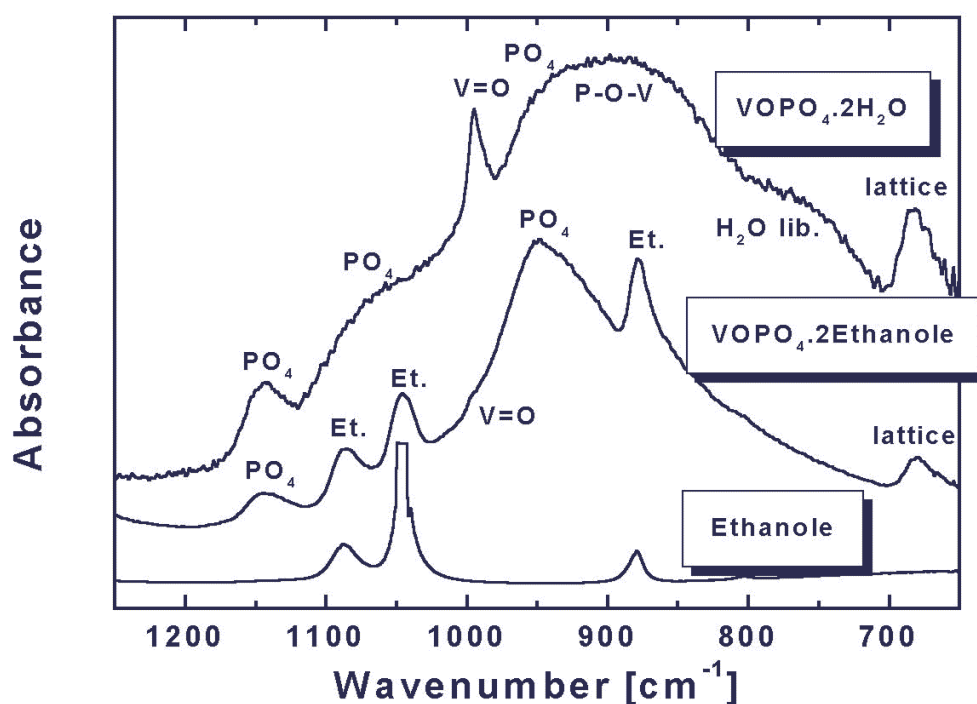


Figure 6b IR spectra of the host structure $\text{VOPO}_4 \cdot 2\text{H}_2\text{O}$, intercalate $\text{VOPO}_4 \cdot 2\text{C}_2\text{H}_5\text{OH}$ and ethanole



First of all, the comparison of IR and Raman spectra for the host compound, intercalate and guest species is very important support of the modelling strategy. Rigid units can be assigned in the initial model on the base of this comparison.

The results of modelling enable the interpretation of vibrational spectra and the explanation of changes due to the intercalation, such as the changes in hydrogen bonding scheme in the interlayer and disorder in interlayer structure. This disorder is manifested by the broadening of spectral bands, as a result of bond distance fluctuations for certain bonds.

Present results showed that the diffraction method and vibrational spectroscopy (IR and Raman) represent complementary experimental method to molecular simulations in complex structure analysis of intercalates and all partially disordered structures.

Acknowledgements This work was supported by the grant agency GACR grant no: 203/97/1010 and grant agency GAUK grant no: 37/97/B.

References

1. Clearfield, A. (Ed.) *Inorganic Ion Exchange Material*; CRC Press, Inc. Boca Raton, Florida: **1982**, Chapters 1,2,3.
2. Alberti, G. in *Recent Developments in Ion Exchange*; Williams, P.A. ; Hudson, M. J. (Ed); Elsevier Applied Science; London **1987**, pp 233.
3. Costantino, U. *J. Chem. Soc. Dalton Trans.* **1979**, 402.
4. Čapková, P.; Beneš, L.; Melánová, K.; Schenk, H. *J. Appl. Cryst.* **1998**, in print.
5. Čapková, P.; Janeba D.; Beneš, L.; Melánová, K.; Schenk, H. *J. Mol. Model.* **1998**, 4, 150.
6. Mayo, L. S.; Olafson, B. D.; Goddard III, W. A. *J. Phys. Chem.* **1990**, 94, 8897.
7. Karasawa, N.; Goddard III, W. A. *J. Phys. Chem.* **1989**, 93, 7320.
8. Rappé, A. K.; Goddard III, W. A. *J. Phys. Chem.* **1991**, 95, 3358.
9. Clearfield, A.; Smith, D. G. *Inorg. Chem.* **1969**, 8, 431.
10. Troup, J. M.; Clearfield, A. *Inorg. Chem.* **1977**, 16, 3311.
11. Tachez, M.; Theobald, F.; Bernard, J.; Hewat, A. W. *Revue de Chemie Minerale* **1982**, 19, 291.
12. Tietze, H. R. A. *J. Chem.* **1981**, 34, 2035.
13. Ross S. D. *Inorganic Infrared and Raman Spectra*, McGraw-Hill, London **1972**.
14. Chauvel, A.; de Roy, M. E.; Besse, J. P.; Benarbia, A.; Legrouri, A.; Barroug, A. *Materials Chemistry and Physics* **1995**, 40, 207.
15. Antonio, M. R.; Barbour, R. L.; Blum, P. R. *Inorg. Chem.* **1987**, 26, 1235
16. Rappe, A. K.; Casewit, C.J.; Colwell, K.S.; Goddard-III, W.A.; Skiff, W. M. *J. Am. Chem. Soc.* **1992**, 114, 10024.
17. Trchová, M.; Melánová, K.; Beneš, L.; Matějka, P.; Uhlířová, E.; Klimovič, J. *Inorg. Chem.* **1998**, submitted.